NEUTRON STAR MERGER

Light curves of the neutron star merger GW170817/SSS17a: Implications for r-process nucleosynthesis

M. R. Drout,[1]* A. L. Piro,[1] B. J. Shappee,[1,2] C. D. Kilpatrick,[3] J. D. Simon,[1] C. Contreras,[4] D. A. Coulter,[3] R. J. Foley,[3] M. R. Siebert,[3] N. Morrell,[4] K. Boutsia,[4] F. Di Mille,[4] T. W.-S. Holoien,[1] D. Kasen,[5,6] J. A. Kollmeier,[1] B. F. Madore,[1] A. J. Monson,[1,7] A. Murguia-Berthier,[3] Y.-C. Pan,[3] J. X. Prochaska,[3] E. Ramirez-Ruiz,[3,8] A. Rest,[9,10] C. Adams,[11] K. Alatalo,[1,9] E. Bañados,[1] J. Baughman,[12,13] T. C. Beers,[14,15] R. A. Bernstein,[1] T. Bitsakis,[16] A. Campillay,[17] T. T. Hansen,[1] C. R. Higgs,[18,19] A. P. Ji,[1] G. Maravelias,[20] J. L. Marshall,[21] C. Moni Bidin,[22] J. L. Prieto,[13,23] K. C. Rasmussen,[14,15] C. Rojas-Bravo,[3] A. L. Strom,[1] N. Ulloa,[17] J. Vargas-González,[4] Z. Wan,[24] D. D. Whitten[14,15]

On 17 August 2017, gravitational waves (GWs) were detected from a binary neutron star merger, GW170817, along with a coincident short gamma-ray burst, GRB 170817A. An optical transient source, Swope Supernova Survey 17a (SSS17a), was subsequently identified as the counterpart of this event. We present ultraviolet, optical, and infrared light curves of SSS17a extending from 10.9 hours to 18 days postmerger. We constrain the radioactively powered transient resulting from the ejection of neutron-rich material. The fast rise of the light curves, subsequent decay, and rapid color evolution are consistent with multiple ejecta components of differing lanthanide abundance. The late-time light curve indicates that SSS17a produced at least ~0.05 solar masses of heavy elements, demonstrating that neutron star mergers play a role in rapid neutron capture (r-process) nucleosynthesis in the universe.

The discovery of gravitational waves (GWs) from coalescing binary black holes by the Laser Interferometer Gravitational Wave Observatory (LIGO) has transformed the study of compact objects in the universe (*1*, *2*). Unlike black holes, merging neutron stars are expected to produce electromagnetic radiation. The electromagnetic signature of such an event can provide more information than the GW signal alone: constraining location of the source, reducing the degeneracies in GW parameter estimation (*3*), probing the expansion rate of the universe (*4*, *5*), and producing a more complete picture of the merger process (*6*, *7*).

Short gamma-ray bursts (GRBs) have long been expected to result from neutron star mergers (*8*, *9*) and therefore would be a natural electromagnetic counterpart to GWs (*10*). Unfortunately, their emission is beamed, so that it may not intersect our line of sight (*11*). The possibility that only a small fraction of GRBs may be detectable has motivated theoretical and observational searches for more-isotropic electromagnetic signatures, such as an astronomical transient powered by the radioactive decay of neutron-rich ejecta from the merger (*12*–*17*). The detection of these events, referred to as macronovae or kilonovae, would provide information on the origin of many of the heaviest elements in the periodic table (*18*).

It has long been realized that about half of the elements heavier than iron are created via rapid neutron capture (r-process) nucleosynthesis—the capture of neutrons onto lighter seed nuclei on a time scale more rapid than β-decay pathways (*19*, *20*). However, it is less clear where the r-process predominantly occurs, namely whether the primary sources of these elements are core-collapse supernovae or compact binary mergers (black hole–neutron star or neutron star–neutron star) (*21*–*23*). For supernovae, direct detection of the electromagnetic signatures from r-process nucleosynthesis is obscured by the much larger luminosity originating from hydrogen recombination (for hydrogen-rich supernovae) or nickel-56 and cobalt-56 decay (for hydrogen-poor supernovae). By contrast, it may be possible to measure the r-process nucleosynthesis after a compact object merger from the associated transient, based on its radioactive decay. Such a measurement would demonstrate directly that r-process elements are produced in compact mergers and provide an estimate of the r-process yield. Although there has been some tentative evidence for kilonovae following short gamma-ray bursts (*24*, *25*), no conclusive event has yet been observed.

Ultraviolet, optical, and infrared observations of a neutron star merger

On 17 August 2017, the LIGO and Virgo interferometers jointly detected and localized the gravitational wave source GW170817, which was identified as a binary neutron star merger based on the waveform (*26*–*28*). At 23:33 UTC on 17 August 2017 (10.86 hours postmerger), an optical transient, Swope Supernova Survey 2017a (SSS17a), was identified in the galaxy NGC 4993 by the 1M2H collaboration and was determined to be associated with this event (*29*, *30*). Within an hour of the identification, we began observing the spectral energy distribution (SED) of SSS17a from the optical to near-infrared (near-IR) with the Magellan telescopes (*31*). Early spectra of the source, also obtained within an hour of the optical discovery, were blue and smooth, indicating that the transient event was initially very hot (*32*, *33*). Over the following weeks, we acquired optical and near-IR imaging of SSS17a at Las Campanas Observatory and W. M. Keck Observatory with the Swope, du Pont, Magellan, and Keck-I telescopes, which are analyzed below (*34*). A companion paper presents optical spectroscopy of SSS17a for an overlapping time period (*33*). Figure 1A shows the discovery image, composed of data obtained with the Magellan/Swope telescopes on the night of 17 August with *g*-, *i*-, and *H*-band spectral filters (transmission functions for all broadband filters used in this manuscript are summarized in Fig. 3B). For comparison, Fig. 1B shows a color image from observations obtained 4 days later. The change in color of SSS17a between these images demonstrates the rapid evolution of this transient.

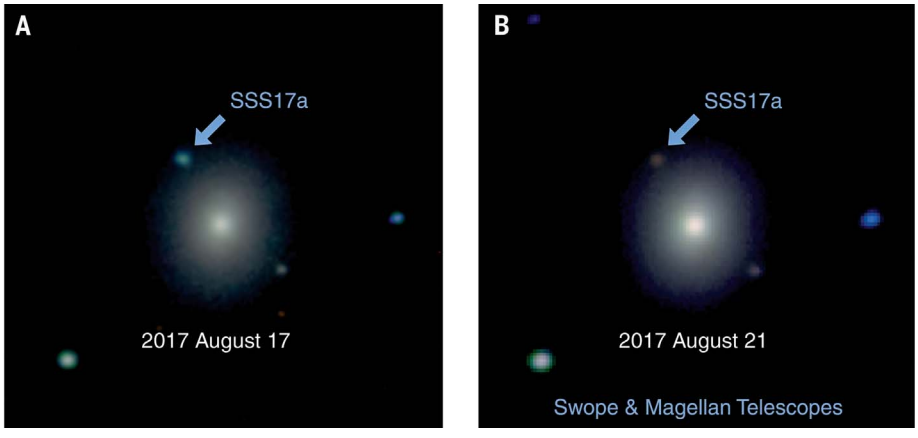

Fig. 1. Pseudocolor images of SSS17a in the galaxy NGC 4993. Images are 1 by 1 arcminutes and centered on NGC 4993; SSS17a is indicated by a blue arrow in each panel. The red, green, and blue channels correspond to the *H*-, *i*-, and *g*-band images described in (*33*). (**A**) Images taken on the night of 17 August 2017, 0.5 days after the merger. (**B**) Images taken on the night of 21 August 2017, 4.5 days after the merger. Over 4 days, SSS17a both faded and became redder.

The resulting light curves are shown in Fig. 2, augmented with measurements made from public *Swift* imaging at ultraviolet (UV) wavelengths, and European Southern Observatory (ESO) images in the optical and near-IR (*33*). SSS17a undergoes a rapid rise on a time scale that varies with wavelength, from <12 hours in the UV and optical bands, to 1 to 2 days in the near-IR. Over subsequent days, the transient fades quickly. This decline proceeds most rapidly in the bluest bands, where SSS17a fades by $\gtrsim 1.5$ mag day^{-1}, but more slowly in the near-IR, where a ~3.5 magnitude decline takes nearly 3 weeks. After correcting for foreground Milky Way reddening (*34*) and the distance to NGC 4993 of 39.5 megaparsecs (Mpc), we find that SSS17a has a peak magnitude of –16.04 mag in the optical (*V*-band) and –15.51 mag in the near-IR (*H*-band) and undergoes a large color evolution. Between 0.5 and 4.5 days postmerger, the *V* minus *H* color of SSS17a transitions from –1.2 mag to +3.6 mag (fig. S1). Although SSS17a reaches absolute magnitudes typically associated with faint core-collapse supernovae, it both declines in magnitude and evolves to redder colors more rapidly than known optical extragalactic transients (*34*, *35*).

Energetics, explosion parameters, and ejecta properties of SSS17a

We construct UV to near-IR SEDs for SSS17a at 10 epochs between 0.5 and 8.5 days after the gravitational wave trigger (Fig. 3). Within 8 days, the peak of the SED falls by a factor of $\gtrsim 70$ in flux and shifts from the near-UV ($\lesssim$4500 Å) to the near-IR ($\gtrsim 1.5$ μm). The SED at each epoch can be fitted with a blackbody distribution (reduced $\chi^2 \sim 1$ to 2), so we consider that the emission is largely thermal. Some deviations are present, most notably an excess in the *Y*-band spectral filter (central wavelength ~1 μm present from day 1.5 onward (*34*). The associated color temperatures show that between 12 and 36 hours postmerger, SSS17a cooled from ~10,000 K to ~5,100 K. Between 0.5 and 5.5 days postmerger, the evolution of the color temperature (T_c) with time (t) is consistent with a power-law decline: $T_c \propto t^{-0.54\pm0.01}$. After 5.5 days, the temperature asymptotically approached ~2500 K.

Using the SEDs from each epoch shown in Fig. 3, we construct a pseudobolometric light curve, which accounts for flux across the electromagnetic spectrum. We compute and sum the SED fluxes using an iterative technique (*34*). To account for flux outside the range of our observations, we extrapolate blackbody emission based on our best-fitting distributions. For flux at shorter wavelengths than our data, the correction factor is ~40% at 0.5 days—because the temperature is hottest and our observations are limited to wavelengths $\lambda \gtrsim 4500$ Å—but it falls below 1% by 0.67 days, when *Swift* Ultraviolet/Optical Telescope (UVOT) observations begin and the transient rapidly cools. The complementary correction factor for flux at longer wavelengths than our near-IR observations ranges from ~1% at day 0.5 to 38% at day 8.5. We plot the resulting pseudobolometric light curve in Fig. 4A. The lower limits of the error bars show the amount of flux that we directly observed. In Fig. 4C, we combine our fitted temperatures with the bolometric luminosity (L_{bol}) to estimate an effective photospheric radius (R_{phot}).

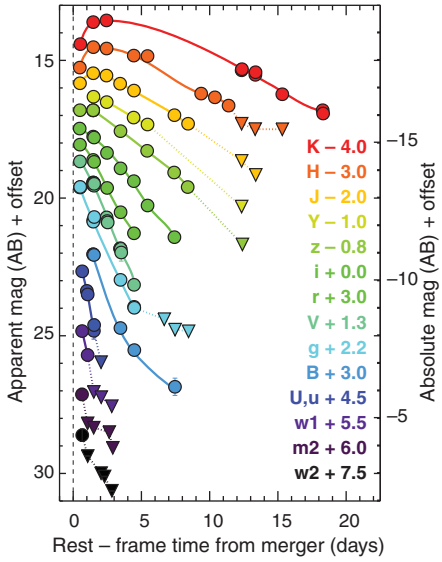

Fig. 2. UV to near-IR photometry of SSS17a. Observations begin 10.9 hours after merger and continue to +18.5 rest-frame days. SSS17a exhibits both a rapid rise and a rapid decline and becomes substantially redder with time. Detections are shown as circles and connected by solid lines for a given photometric band. Upper limits are shown as triangles and connected by dotted lines. The time of merger is indicated by a vertical dashed line. The right-hand vertical axis accounts only for the distance to the host galaxy, NGC 4993. For absolute magnitudes corrected for foreground Milky Way reddening, see (*34*).

For observations >8.5 days after the merger, we only detect the source in either *H*- or *K*-band near-IR images at any given time, so we cannot directly measure the temperature. To estimate bolometric luminosities and photospheric radii at these later epochs, we assume an effective temperature of 2500^{+500}_{-1000} K. Although the physical motivation for this choice is further detailed below, observationally, the measurable color temperature is approaching this value from 5.5 to 8.5 days postmerger. Further, the *H*- and *K*-bands fall near the peak of the SED for blackbodies in the temperature range 1500 to 3000 K. As a result, bolometric corrections for either the *H*- or *K*-bands over this entire temperature range lead to a variation in the estimated luminosity of less than a factor of 1.6. Error bars representing this full range are included in Fig. 4, A and C.

The pseudo-bolometric light curve has a peak value of ~10^{42} erg s^{-1} at 0.5 days postmerger, corresponding to our first epoch of observations, and the total radiated energy over 18 days is ~1.7×10^{47} erg. Between 0.5 and 5.5 days postmerger, the bolometric light curve is consistent with a power-law decline of $L_{bol} \propto t^{-0.85\pm0.01}$. After 5.5 days, the best-fitting power law is steeper, with $L_{bol} \propto t^{-1.33\pm0.15}$ between 7.5 and 13.5 days.

The energy source powering SSS17a

We use the evolution of L_{bol}, T_c, and R_{phot} to constrain the energy source powering the emission from SSS17a. We first explore whether the physical properties of SSS17a are consistent with a transient powered by the radioactive decay of r-process elements. Models for r-process powered transients predict that the energy generation rate, $\dot{q}_r$, is proportional to $t^{-1.3}$ (*14*, *15*, *34*). This power law is similar to the slope observed in the late-time bolometric light curve of SSS17a. To directly compare the predictions for r-process heating to our observed luminosities, we multiply this intrinsic heating rate by a time-dependent thermalization efficiency (60 to 25%) (*34*) and fit our data. According to Arnett's law, the peak luminosity of a radioactively powered transient should correspond to the instantaneous heating rate (*36*). Under the hypothesis that the luminosity at 0.5 days postmerger is due to r-process heating, this implies that ~0.01 solar masses ($M_\odot$) of r-process material was generated. The heating

[1]The Observatories of the Carnegie Institution for Science, 813 Santa Barbara Street, Pasadena, CA 91101, USA. [2]Institute for Astronomy, University of Hawai'i, 2680 Woodlawn Drive, Honolulu, HI 96822, USA. [3]Department of Astronomy and Astrophysics, University of California, Santa Cruz, CA 95064, USA. [4]Las Campanas Observatory, Carnegie Observatories, Casilla 601, La Serena, Chile. [5]Departments of Physics and Astronomy, 366 LeConte Hall, University of California, Berkeley, CA 94720, USA. [6]Nuclear Science Division, Lawrence Berkeley National Laboratory, Berkeley, CA 94720, USA. [7]Department of Astronomy and Astrophysics, The Pennsylvania State University, 525 Davey Laboratory, University Park, PA 16802, USA. [8]Dark Cosmology Center, Niels Bohr Institute, University of Copenhagen, Blegdamsvej 17, 2100 Copenhagen, Denmark. [9]Space Telescope Science Institute, 3700 San Martin Drive, Baltimore, MD 21218, USA. [10]Department of Physics and Astronomy, The Johns Hopkins University, 3400 North Charles Street, Baltimore, MD 21218, USA. [11]Division of Physics, Mathematics, and Astronomy, California Institute of Technology, Pasadena, CA 91125, USA. [12]Massachusetts Institute of Technology, Cambridge, MA, USA. [13]Núcleo de Astronomía de la Facultad de Ingeniería y Ciencias, Universidad Diego Portales, Avenida Ejército 441, Santiago, Chile. [14]Department of Physics, University of Notre Dame, Notre Dame, IN 46556, USA. [15]Joint Institute for Nuclear Astrophysics, Center for the Evolution of the Elements, East Lansing, MI 48824, USA. [16]Instituto de Radioastronomía y Astrofísica, Universidad Nacional Autónoma de México, C.P. 58190, Morelia, Mexico. [17]Departamento de Física y Astronomía, Facultad de Ciencias, Universidad de La Serena, Cisternas 1200, La Serena, Chile. [18]University of Victoria, Victoria, British Columbia, Canada. [19]National Research Council Herzberg Institute of Astrophysics, 5071 West Saanich Road, Victoria, British Columbia V9E 2E7, Canada. [20]Instituto de Física y Astronomía, Universidad de Valparaíso, Avenida Gran Bretaña 1111, Casilla 5030, Valparaíso, Chile. [21]George P. and Cynthia Woods Mitchell Institute for Fundamental Physics and Astronomy, and Department of Physics and Astronomy, Texas A&M University, College Station, TX 77843, USA. [22]Instituto de Astronomía, Universidad Católica del Norte, Avenida Angamos 0610, Antofagasta, Chile. [23]Millennium Institute of Astrophysics, Santiago, Chile. [24]Sydney Institute for Astronomy, School of Physics, A28, University of Sydney, NSW 2006, Australia.
***Corresponding author. Email: mdrout@carnegiescience.edu**

rate for this mass of r-process material, M_{r-p}, is plotted in Fig. 4A.

Although heating from ~0.01 $M_\odot$ of r-process ejecta could explain the peak observed luminosity, it would have several further consequences. First, the fast rise (<0.5 days) would require that the specific opacity, κ, of this material be less than ~0.08 $cm^2\ g^{-1}$ (*34*). The opacity is strongly dependent on the presence of lanthanide elements, because they have a large number of bound-bound transitions due to the presence of an open *f* shell (*37*). This low inferred opacity would thus imply that the early ejecta cannot be lanthanide-rich. Then, the abundance of lanthanides is strongly dependent on the neutron richness of the ejecta, often expressed as the electron fraction Y_e, where $Y_e = 0.5$ for symmetric matter (equal proportions of neutrons and protons) and $Y_e = 0$ for pure neutrons. To produce material with such low opacity that is relatively lanthanide-free would require $Y_e \gtrsim 0.3$.

Second, this low inferred opacity would cause the associated material to quickly become optically thin (within ~2 days, when SSS17a is blue/hot). A low optical depth is inconsistent with the continuing optical emission that we observed over the following weeks from SSS17a, so this model necessitates an additional higher-opacity component. Comparing the r-process heating to the later light curve yields a mass estimate of $0.05 \pm 0.02\ M_\odot$ (Fig. 4A), but for SSS17a to remain optically thick for a time scale of 2 to 3 weeks requires an opacity $\kappa \gtrsim 5 cm^3 g^{-1}$. The evolution of the light curve over this time interval therefore constitutes evidence for a second, lanthanide-rich component, which dominates at later times when the SSS17a is red/cool.

Such two-component ejecta are generally expected for neutron star mergers (*38*, *39*). This structure could correspond to two distinct physical components, where the lanthanide-rich component arises from material ejected on dynamical time scales via processes such as tidal forces (*40*) and the lanthanide-free component forms on longer time scales (~seconds), such as from the accretion disk wind (*41*). Alternatively, both of these compositional components could arise from the same dynamical ejecta (*42*, *43*). The exact contribution of each component to the observed light curve depends on the mass ratio of the merging binary, as well as the orientation relative to the line of sight (*44*). For example, it is possible that the blue component could be underestimated if it is partially obscured/absorbed by the material producing the red component. Detailed modeling, which accounts for these degeneracies, is presented in a companion paper (*45*).

Figure 4C shows the evolution of the measured radii. A comparison to model curves for material moving at 10, 20, and 30% of the speed of light indicates that the photosphere expands at relativistic speeds in the first few days. However, after about 5 days, the photosphere begins moving inward. This behavior is reminiscent of hydrogen-rich core-collapse supernovae after hydrogen recombination (*46*), and a similar process may be occurring here. In the case of an r-process powered transient, recombination of the open *f*-shell lanthanide elements, such as neodymium, is expected to begin at a temperature of ~2500 K (*37*). These ionized elements are the dominant opacity source, so the recombination causes the opacity to decline rapidly and the photosphere to move inward. This interpretation is corroborated by the effective temperature of ~2500 K that we measure from the SED for $t > 5$ days and supports our assumption of a roughly constant temperature throughout the remainder of the evolution.

Other processes have been considered for providing an optical counterpart to neutron star mergers, including magnetic dipole spin-down, heating from radioactive nickel, and cocoon emission [e.g., (*47*–*49*)]. These models must be compared with our detailed observations as well. For instance, luminosity powered by the spin-down

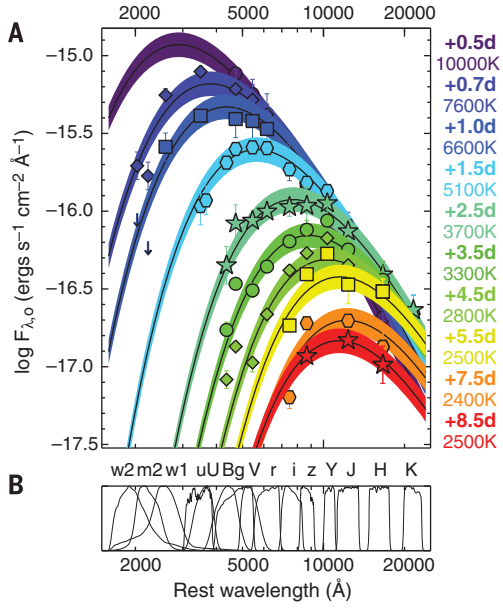

Fig. 3. Evolution of the UV to near-IR SED of SSS17a. (**A**) The vertical axis, log $F_{\lambda,o}$, is the logarithm of the observed flux. Fluxes have been corrected for foreground Milky Way extinction (*34*). Detections are plotted as filled symbols, and upper limits for the third epoch (1.0 days postmerger) as downward pointing arrows. Less-constraining upper limits at other epochs are not plotted for clarity. Between 0.5 and 8.5 days after the merger, the peak of the SED shifts from the near-UV (<4500 Å) to the near-IR (>1 μm) and fades by a factor >70. The SED is broadly consistent with a thermal distribution, and the colored curves represent best-fitting blackbody models at each epoch. In 24 hours after the discovery of SSS17a, the observed color temperature falls from ≳ 10,000 K to ~5000 K. The epoch and best-fitting blackbody temperature (rounded to 100 K) are listed. SEDs for each epoch are also plotted individually in fig. S2 and described in (*34*). (**B**) Filter transmission functions for the observed photometric bands.

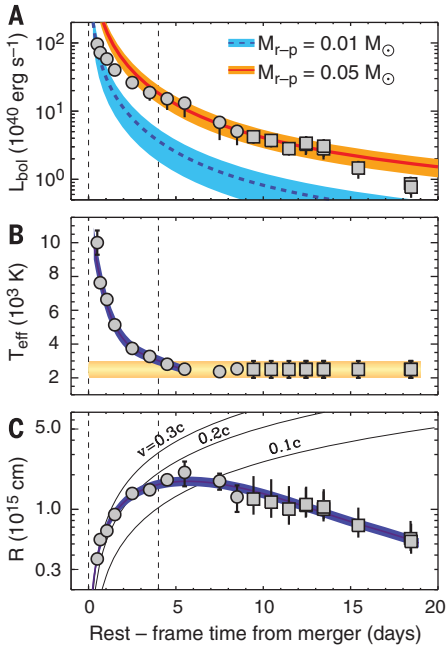

Fig. 4. Physical parameters derived from the UV to near-IR SEDs of SSS17. Vertical dashed lines indicate the time of merger and 4 days postmerger, between which SSS17a undergoes a period of rapid expansion and cooling. (**A**) Pseudo-bolometric light curve evolution; representative r-process radioactive heating curves are also shown. Although the initial observed peak is consistent with ~0.01 $M_\odot$ of r-process material (blue curve), this underpredicts the luminosity at later times. Instead, the late-time (>4 days) light curve matches radioactive heating from $0.05 \pm 0.02\ M_\odot$ of r-process material (red curve). (**B**) Best-fitting blackbody model temperatures. At 11 hours after the merger, SSS17a is consistent with a blackbody of ≳ 10,000 K. Between 4.5 and 8.5 days, the temperature asymptotically approaches ~2500 K, the temperature at which open *f*-shell lanthanide elements are expected to recombine. Radii and luminosities beyond 8.5 days are computed assuming a temperature of 2500^{+500}_{-1000} K and are plotted as squares. This temperature range is highlighted by the orange horizontal band. (**C**) Best-fitting blackbody model radii. Curved lines represent the radius of material moving at 10, 20, and 30% the speed of light. At early times the increase in radius with time implies that the ejecta are expanding relativistically. After ~5 days, the measured radii decrease, likely due to recombination.

of a magnetic dipole is predicted to scale as $L_{bol} \propto t^{-2}$, steeper than the measured bolometric light curve of SSS17a, and should produce strong x-ray emission (*47*). Then, similar to r-process heating, power from radioactive nickel cannot self-consistently reproduce the entire photometric evolution of SSS17a; fitting both the peak luminosity and fast decline leads to the unphysical requirement that the mass of radioactive nickel approaches or exceeds the total ejecta mass (*34*). Still, we find that it is possible to reproduce the bolometric evolution between 7.5 and 18 days postmerger with heating due to ~0.002 $M_\odot$ of radioactive nickel (*34*) if another emission process dominates at early times. However, nickel heating does not naturally explain the temperature evolution observed in SSS17a. A rapid evolution to very red colors is not observed in other known transients powered by radioactive nickel (*35*).

Implications for r-process nucleosynthesis

We conclude that the late-time ($\gtrsim$ 5 days) decay rate and color evolution of SSS17a are consistent with a transient powered by the radioactive decay of r-process elements. If the early emission is also powered by r-process heating, multiple ejecta components with differing lanthanide abundances are required. Overall, we estimate that at least ~0.05 $M_\odot$ of r-process material is generated in this event from the late-time light curve.

The predicted mass fraction of lanthanides in this material is ~0.1 to 0.5, depending on Y_e (*42*). Typical solar abundance (by mass fraction) for the r-process elements with mass number $A > 100$ is ~8×10^{-8} (*50*), resulting in a Milky Way r-process production rate of ~$3 \times 10^{-7}\ M_\odot\ \mathrm{year}^{-1}$ (*48*, *51*). If neutron star mergers dominate r-process production, this production rate requires an event like GW170817/SSS17a in our Galaxy every 20,000 to 80,000 years, or a volume density of ~(1 to 4) × $10^{-7}\ \mathrm{Mpc}^{-3}\ \mathrm{year}^{-1}$. At their design sensitivity, Advanced LIGO, Advanced Virgo, and the Kamioka Gravitational Wave Detector (KAGRA) will be able to detect binary neutron star mergers out to 200 Mpc (*52*), leading to a possible detection rate of ~3 to 12 per year. This rate translates to less than one event per year as nearby as GW170817/SSS17a. This number would increase if the r-process mass that we calculate for SSS17a is overestimated. Such an overestimate could occur if our assumed heating efficiency is too low or if this event produced more ejecta than an average neutron star merger.

Empirical explanation for the portion of the periodic table expected to result from r-process nucleosynthesis has been elusive. The UV to near-IR light curves of the neutron star merger GW170817/SSS17a provide evidence for binary neutron star mergers as an origin for these elements. Observations of more events are now required to precisely map r-process yields from this channel.

REFERENCES AND NOTES

1. LIGO Scientific Collaboration and Virgo Collaboration, *Phys. Rev. X* **6**, 041015 (2016).
2. LIGO Scientific Collaboration and Virgo Collaboration, *Phys. Rev. Lett.* **116**, 061102 (2016).
3. S. A. Hughes, D. E. Holz, *Class. Quantum Gravity* **20**, S65–S72 (2003).
4. D. E. Holz, S. A. Hughes, *Astrophys. J.* **629**, 15–22 (2005).
5. S. Nissanke *et al.*, arXiv:astro-ph/1307.2638 [astro-ph.CO] (10 July 2013).
6. E. S. Phinney, arXiv:astro-ph/0903.0098 [astro-ph.CO] (28 February 2009).
7. I. Mandel, R. O'Shaughnessy, *Class. Quantum Gravity* **27**, 114007 (2010).
8. B. Paczynski, *Astrophys. J.* **308**, L43 (1986).
9. D. Eichler, M. Livio, T. Piran, D. N. Schramm, *Nature* **340**, 126–128 (1989).
10. L. Z. Kelley, I. Mandel, E. Ramirez-Ruiz, *Phys. Rev. D Part. Fields Gravit. Cosmol.* **87**, 123004 (2013).
11. W. Fong, E. Berger, R. Margutti, B. A. Zauderer, *Astrophys. J.* **815**, 102 (2015).
12. L.-X. Li, B. Paczyński, *Astrophys. J.* **507**, L59–L62 (1998).
13. S. R. Kulkarni, arXiv:astro-ph/0510256 [astro-ph.CO] (10 October 2005).
14. B. D. Metzger *et al.*, *Mon. Not. R. Astron. Soc.* **406**, 2650–2662 (2010).
15. L. F. Roberts, D. Kasen, W. H. Lee, E. Ramirez-Ruiz, *Astrophys. J.* **736**, L21 (2011).
16. T. Piran, E. Nakar, S. Rosswog, *Mon. Not. R. Astron. Soc.* **430**, 2121–2136 (2013).
17. B. D. Metzger, *Living Rev. Relativ.* **20**, 3 (2017).
18. S. Shen *et al.*, *Astrophys. J.* **807**, 115 (2015).
19. E. M. Burbidge, G. R. Burbidge, W. A. Fowler, F. Hoyle, *Rev. Mod. Phys.* **29**, 547–650 (1957).
20. A. G. W. Cameron, *Publ. Astron. Soc. Pac.* **69**, 201 (1957).
21. J. M. Lattimer, D. N. Schramm, *Astrophys. J.* **192**, L145 (1974).
22. Y.-Z. Qian, G. J. Wasserburg, *Phys. Rep.* **442**, 237–268 (2007).
23. M. Arnould, S. Goriely, K. Takahashi, *Phys. Rep.* **450**, 97–213 (2007).
24. N. R. Tanvir *et al.*, *Nature* **500**, 547–549 (2013).
25. E. Berger, W. Fong, R. Chornock, *Astrophys. J.* **774**, L23 (2013).
26. LIGO/Virgo Collaboration, *GRB Coordinates Network* **21509** (2017).
27. LIGO/Virgo Collaboration, *GRB Coordinates Network* **21513** (2017).
28. B. P. Abbott, *Phys. Rev. Lett.* **119**, 161101 (2017).
29. One-Meter Two-Hemisphere (1M2H) Collaboration, *GRB Coordinates Network* **21529** (2017).
30. D. A. Coulter *et al.*, *Science* **358**, 1556–1558 (2017).
31. J. D. Simon *et al.*, *GRB Coordinates Network* **21551** (2017).
32. M. R. Drout *et al.*, *GRB Coordinates Network* **21547** (2017).
33. B. J. Shappee *et al.*, *Science* **358**, 1574–1578 (2017).
34. Materials and methods are available as supplementary materials.
35. M. R. Siebert *et al.*, *Astrophys. J.* **848**, aa905e (2017).
36. W. D. Arnett, *Astrophys. J.* **253**, 785 (1982).
37. D. Kasen, N. R. Badnell, J. Barnes, *Astrophys. J.* **774**, 25 (2013).
38. A. Perego *et al.*, *Mon. Not. R. Astron. Soc.* **443**, 3134–3156 (2014).
39. R. Fernández, B. D. Metzger, *Annu. Rev. Nucl. Part. Sci.* **66**, 23–45 (2016).
40. K. Hotokezaka *et al.*, *Phys. Rev. D Part. Fields Gravit. Cosmol.* **87**, 024001 (2013).
41. R. Fernández, D. Kasen, B. D. Metzger, E. Quataert, *Mon. Not. R. Astron. Soc.* **446**, 750–758 (2015).
42. S. Wanajo *et al.*, *Astrophys. J.* **789**, L39 (2014).
43. L. Bovard *et al.*, arXiv:astro-ph/1709/09630 [gr-qc] (27 September 2017).
44. D. Kasen, R. Fernández, B. D. Metzger, *Mon. Not. R. Astron. Soc.* **450**, 1777–1786 (2015).
45. C. D. Kilpatrick *et al.*, *Science* **358**, 1583–1587 (2017).
46. A. Elmhamdi *et al.*, *Mon. Not. R. Astron. Soc.* **338**, 939–956 (2003).
47. B. D. Metzger, A. L. Piro, *Mon. Not. R. Astron. Soc.* **439**, 3916–3930 (2014).
48. B. D. Metzger, A. L. Piro, E. Quataert, *Mon. Not. R. Astron. Soc.* **396**, 304–314 (2009).
49. O. Gottlieb, E. Nakar, T. Piran, arXiv:astro-ph/1705.10797 [astro-ph.HE] (30 May 2017).
50. F. Kappeler, H. Beer, K. Wisshak, *Rep. Prog. Phys.* **52**, 945–1013 (1989).
51. Y. Qian, *Astrophys. J.* **534**, L67–L70 (2000).
52. LIGO Scientific Collaboration; Virgo Collaboration, *Living Rev. Relativ.* **19**, 1 (2016).
53. J. Guillochon, J. Parrent, L. Z. Kelley, R. Margutti, *Astrophys. J.* **835**, 64 (2017).

ACKNOWLEDGMENTS

We thank J. Mulchaey (Carnegie Observatories), L. Infante (Las Campanas Observatory), and the entire Las Campanas Observatory staff for their dedication, professionalism, and excitement, which were all critical in obtaining the observations used in this study. We also thank I. Thompson and the Carnegie Observatory Time Allocation Committee for approving the Swope Supernova Survey and scheduling our program. We thank the University of Copenhagen, Dark Cosmology Centre, and the Niels Bohr International Academy for hosting D.A.C., R.J.F., A.M.B., E.R., and M.R.S. during this work. R.J.F., A.M.B., and E.R. were participating in the Kavli Summer Program in Astrophysics, "Astrophysics with gravitational wave detections." This program was supported by the Kavli Foundation, Danish National Research Foundation, the Niels Bohr International Academy, and the Dark Cosmology Centre. M.R.D., B.J.S., K.A.A., and A.P.J. were supported by NASA through Hubble Fellowships awarded by the Space Telescope Science Institute, which is operated by the Association of Universities for Research in Astronomy, Inc., for NASA, under contract NAS 5-26555. M.R.D. is a Hubble and Carnegie-Dunlap Fellow. M.R.D. acknowledges support from the Dunlap Institute at the University of Toronto, and thanks M. W. B. Wilson, L. Z. Kelly, C. McCully, and R. Margutti for helpful discussions. The University of California, Santa Cruz (UCSC) group is supported in part by NSF grant AST-1518052; the Gordon and Betty Moore Foundation; the Heising-Simons Foundation; generous donations from many individuals through a UCSC Giving Day grant; and fellowships from the Alfred P. Sloan Foundation (R.J.F), the David and Lucile Packard Foundation (R.J.F. and E.R.), and the Niels Bohr Professorship from the DNRF (E.R.). D.K. is supported in part by a Department of Energy (DOE) Early Career award DE-SC0008067, a DOE Office of Nuclear Physics award DE-SC0017616, and a DOE SciDAC award DE-SC0018297, and by the Director, Office of Energy Research, Office of High Energy and Nuclear Physics, Divisions of Nuclear Physics, of the U.S. Department of Energy under contract No.DE-AC02-05CH11231. Support for J.L.P. is in part provided by FONDECYT through grant 1151445 and by the Ministry of Economy, Development, and Tourism's Millennium Science Initiative through grant IC120009, awarded to The Millennium Institute of Astrophysics, MAS. C.M.B. was supported by FONDECYT through regular project 1150060. G.M. acknowledges support from CONICYT, Programa de Astronomía/PCI, FONDO ALMA 2014, Proyecto no. 31140024. A.M.B. acknowledges support from a UCMEXUS-CONACYT Doctoral Fellowship. C.A. was supported by the California Institute of Technology through a Summer Undergraduate Research Fellowship (SURF) with funding from the Associates SURF Endowment. T.C.B., K.C.R., and D.D.W. acknowledge partial support for this work from grant PHY 14-30152; Physics Frontier Center/Joint Institute for Nuclear Astrophysics Center for the Evolution of the Elements (JINA-CEE), awarded by the U.S. National Science Foundation, and from the Luksic Foundation. J.X.P. is also affiliated with the Kavli Institute for the Physics and Mathematics of the Universe. This paper includes data gathered with the 6.5-m Magellan Telescopes located at Las Campanas Observatory, Chile. This work is based in part on observations collected at the European Organisation for Astronomical Research in the Southern Hemisphere, Chile, as part of PESSTO (the Public ESO Spectroscopic Survey for Transient Objects Survey) through ESO program 199.D-0143. Some of the data presented herein were obtained at the W. M. Keck Observatory, which is operated as a scientific partnership among the California Institute of Technology, the University of California, and NASA. The Observatory was made possible by the generous financial support of the W. M. Keck Foundation. The authors wish to recognize and acknowledge the very important cultural role and reverence that the summit of Maunakea has always had within the indigenous Hawaiian community. We are most fortunate to have the opportunity to conduct observations from this mountain. This research has made use of the NASA/IPAC Extragalactic Database (NED) which is operated by the Jet Propulsion Laboratory, California Institute of Technology, under contract with NASA. This publication makes use of data products from the Two Micron All Sky Survey, which is a joint project of the University of Massachusetts and the Infrared Processing and Analysis Center/California Institute of Technology, funded by NASA and NSF. The Magellan/du Pont data presented in this work and code used

to perform the analysis are available via http or anonymous ftp at [http|ftp]://data.obs.carnegiescience.edu/SSS17a. The Swope data of SSS17a are available at https://ziggy.ucolick.org/sss17a/. ESO and *Swift*-UVOT data analyzed in this work are available at http://archive.eso.org/eso/eso_archive_main.html (program ID 199.D-0143) and https://archive.stsci.edu/swiftuvot/search.php (target IDs 12167, 12978, and 12979), respectively. Reduced photometry is presented in table S1 and is also available on the Open Kilonova Catalog (*53*) (https://kilonova.space).

SUPPLEMENTARY MATERIALS

www.sciencemag.org/content/358/6370/1570/suppl/DC1
Materials and Methods
Figs. S1 to S3
Tables S1 and S2
References (*54*–*89*)

20 September 2017; accepted 11 October 2017
Published online 16 October 2017
10.1126/science.aaq0049

Science

Light curves of the neutron star merger GW170817/SSS17a: Implications for r-process nucleosynthesis

M. R. Drout, A. L. Piro, B. J. Shappee, C. D. Kilpatrick, J. D. Simon, C. Contreras, D. A. Coulter, R. J. Foley, M. R. Siebert, N. Morrell, K. Boutsia, F. Di Mille, T. W.-S. Holoien, D. Kasen, J. A. Kollmeier, B. F. Madore, A. J. Monson, A. Murguia-Berthier, Y.-C. Pan, J. X. Prochaska, E. Ramirez-Ruiz, A. Rest, C. Adams, K. Alatalo, E. Bañados, J. Baughman, T. C. Beers, R. A. Bernstein, T. Bitsakis, A. Campillay, T. T. Hansen, C. R. Higgs, A. P. Ji, G. Maravelias, J. L. Marshall, C. Moni Bidin, J. L. Prieto, K. C. Rasmussen, C. Rojas-Bravo, A. L. Strom, N. Ulloa, J. Vargas-González, Z. Wan and D. D. Whitten

Science **358** (6370), 1570-1574.
DOI: 10.1126/science.aaq0049originally published online October 16, 2017

Photons from a gravitational wave event

Two neutron stars merging together generate a gravitational wave signal and have also been predicted to emit electromagnetic radiation. When the gravitational wave event GW170817 was detected, astronomers rushed to search for the source using conventional telescopes (see the Introduction by Smith). Coulter *et al.* describe how the One-Meter Two-Hemispheres (1M2H) collaboration was the first to locate the electromagnetic source. Drout *et al.* present the 1M2H measurements of its optical and infrared brightness, and Shappee *et al.* report their spectroscopy of the event, which is unlike previously detected astronomical transient sources. Kilpatrick *et al.* show how these observations can be explained by an explosion known as a kilonova, which produces large quantities of heavy elements in nuclear reactions.

Science, this issue p. 1556, p. 1570, p. 1574, p. 1583; see also p. 1554

Science (print ISSN 0036-8075; online ISSN 1095-9203) is published by the American Association for the Advancement of Science, 1200 New York Avenue NW, Washington, DC 20005. The title *Science* is a registered trademark of AAAS.

Science (print ISSN 0036-8075; online ISSN 1095-9203) is published by the American Association for the Advancement of Science, 1200 New York Avenue NW, Washington, DC 20005. The title *Science* is a registered trademark of AAAS.